Solid State Ionics xxx (xxxx) xxx–xxx

Contents lists available at ScienceDirect

Solid State Ionics

journal homepage: www.elsevier.com/locate/ssi

Local disorder and water uptake in $La_{1-x}Sr_xScO_{3-\delta}$

A.S. Farlenkov[a,b,*], A.G. Smolnikov[a,c], M.V. Ananyev[a,b], A.V. Khodimchuk[a,b], A.L. Buzlukov[c], A.V. Kuzmin[a,b], N.M. Porotnikova[a,b]

[a] Institute of High Temperature Electrochemistry of the Ural Branch of the Russian Academy of Sciences, Yekaterinburg 620137, Russia
[b] Ural Federal University named after the first President of Russia B.N. Yeltsin, Yekaterinburg 620002, Russia
[c] M.N. Mikheev Institute of Metal Physics of the Ural Branch of the Russian Academy of Sciences, Yekaterinburg 620990, Russia

ARTICLE INFO

Keywords:
$LaScO_3$
TGA
Water uptake
NMR
Protonics

ABSTRACT

Structure of perovskite oxides $La_{1-x}Sr_xScO_{3-\delta}$ (x = 0, 0.04, 0.09) have been studied by X-Ray powder diffraction method. Orthorhombic distortions are found to decrease with increasing of strontium concentration. Water uptake of Sr-doped lanthanum scandates was studied by means of thermogravimetric analysis over the temperature range of 300–950 °C in gas mixture with water and oxygen partial pressure of pH_2O = 0.24 atm and pO_2 = 0.18 atm, respectively. Based on the thermogravimetry data the hydration enthalpy and entropy have been calculated for oxides $La_{1-x}Sr_xScO_{3-\delta}$ (x = 0.04, 0.09). ^{45}Sc nuclear magnetic resonance (NMR) spectra were taken at T = 300 K and external magnetic field H_0 = 11.7 T. ^{45}Sc NMR study revealed that local symmetry around scandium ions in lanthanum scandate was affected by the presence of both strontium and protonic defects. Possible reasons of ^{45}Sc NMR spectra changes have been considered.

1. Introduction

The acceptor-doped perovskite-like oxides have received considerable attention as solid-state proton conductors for a range of potential electrochemical applications, including solid oxide fuel cells (SOFCs), hydrogen electrochemical sensors and pumps [1,2]. Such materials are particularly promising as electrolytes for SOFCs at intermediate temperature (400–700 °C), which alleviate many of the material lifetime and cyclability challenges arising from the very high operation temperature (800–1000 °C) of conventional zirconia-based SOFCs [3].

Some acceptor-doped $A^{III}B^{III}O_3$ perovskite-type oxides such as $LaSc_{0.8}Mg_{0.2}O_{3-\delta}$, $La_{0.9}Sr_{0.1}LuO_{3-\delta}$, $La_{0.9}Ba_{0.1}ErO_{3-\delta}$, $La_{0.9}Sr_{0.1}ScO_{3-\delta}$, as well as others have been reported to have high proton conductivity in the presence of water vapour or hydrogen at high temperatures [4–10]. Among them, $La_{1-x}Sr_xScO_{3-\delta}$ ceramics show high protonic conductivity, which is comparable with the best known yttrium-doped barium zirconate [11–14], suggesting that Sr-doped $LaScO_3$ oxides are promising proton-conducting material.

Only few papers [15–18] are known in which authors determined the structure of $LaScO_3$. Authors of papers [15,18] have characterized the structure of $La_{1-x}Sr_xScO_{3-\delta}$ as orthorhombic perovskite over the temperature range of 25–1000 °C. The structure type of $La_{1-x}Sr_xScO_{3-\delta}$ is identical to undoped $LaScO_3$. Lanthanum ions are surrounded by twelve oxygen ions which are positioned at the centers of edges of pseudo-cubic unit cell. The unit cell of $La_{1-x}Sr_xScO_{3-\delta}$ has two non-equivalent oxygen positions O1 and O2 and the oxygen vacancies are localized exclusively in O2–positions, whereas protons are associated with O1 oxygen positions [15,18].

Authors of papers [4,8,9,19–22] have studied the effects of dopant concentration on the electrical conductivity of acceptor-doped lanthanum scandate. It was shown that $LaScO_3$ possesses the mixed anionic and hole conductivity in dry atmosphere; hole transference numbers decrease with the decreasing of temperature [19]. In humidified oxygen atmosphere the total conductivity increases with increase of water partial pressure, which can be associated with protonic conductivity.

It is well-known that oxygen vacancies induce incorporation of water molecules and formation of OH-defects (one molecule of water can interact with a vacancy and an oxygen ion to form two OH-defects):

$$H_2O + V_O^{\bullet\bullet} + O_O^{\times} = 2OH_O^{\bullet}, \quad (1)$$

where the Kröger–Vink notation is used to describe an oxygen vacancy $V_O^{\bullet\bullet}$, oxygen ions at an oxygen lattice sites $O_O^{\times}$ and OH-defects on oxygen sites $OH_O^{\bullet}$. Notwithstanding the considerable amount of experimental data on lanthanum scandate some issues concerning structural changes caused by water incorporation, preferable positions for protons and vacancies still remain unclear.

This paper we analyze the effects of temperature, dopant concentration on water uptake and crystal structure of $La_{1-x}Sr_xScO_{3-\delta}$ (x = 0, 0.04, 0.09). Proton concentration, hydration enthalpy and entropy for these oxides are obtained by means of Thermogravimetric Analysis

* Corresponding author.
E-mail address: a.farlenkov@yandex.ru (A.S. Farlenkov).

http://dx.doi.org/10.1016/j.ssi.2017.04.018
Received 15 December 2016; Received in revised form 24 April 2017; Accepted 25 April 2017

(TGA). The structural Rietveld refinements of $La_{1-x}Sr_xScO_{3-\delta}$ (x = 0, 0.04, 0.09) were carried out on the powder X-Ray Diffraction (XRD) data in order to calculate a crystal lattice parameters of strontium doped lanthanum scandates. Nuclear magnetic resonance (NMR) studies of the dry and hydrated samples allow us to reveal the local structure changes of $La_{1-x}Sr_xScO_{3-\delta}$ proton-conducting oxides. The obtained results are compared to the known so far experimental data on lanthanum scandate.

2. Experimental

Powders of $La_{1-x}Sr_xScO_{3-\delta}$ (x = 0, 0.04, 0.09) oxides were synthesized using the citric-nitrate technology; all reagents ($La(NO_3)\cdot 6H_2O$, $Sc(NO_3)_3\cdot 4H_2O$, $SrCO_3$) were of a high purity grade (*puriss. spec.*). Standardized alcohol solutions of $La(NO_3)_3$ and $Sc(NO_3)_3$ were prepared for co-precipitation hydroxides. Necessary quantities of solutions were taken and mixed with each other. After that the alcohol solution of ammonia was put into the nitrate mixture until full precipitation. Strontium carbonate was added to the $LaScO_3$ powder in order to obtain Sr-doped $LaScO_3$. Precipitated hydroxides were filtered and dried at the temperature of 105°C in the baker Snol 67/350 LP (Umega, Lithuania). The dried mixture was annealed in ambient air at the temperature of 900°C during 1 h. After presynthesis at the temperature of 900 °C during 1 h, obtained powders were ground and compacted in the form of tablets (diameter ~ 12 mm, thickness ~ 2 mm). The tablets were sintered in ambient air at the temperature of 1500°C during 5 h. After sintering the tablets were milled in a zirconia mortar.

X-Ray powder diffraction (XRD) and structural analysis were carried out by using D/MAX-2200 RIGAKU conventional diffractometer in $Cu_{K\alpha}$-radiation ($\lambda(K_{\alpha 1})$ = 1.54 Å) at room temperature in ambient air. The diffraction patterns were recorded in the 2θ range of 25–85° with steps of 0.02°. The collection time was 3 h for each XRD-pattern. Structural Rietveld refinement of XRD patterns was carried out by means of *FullProf* software [23]. The line shape of the diffraction peaks was generated by a Thompson-Cox-Hastings pseudo-Voigt function and the background was refined by a 5th degree polynomial. The following parameters were refined: background coefficients, zero point, Thompson-Cox-Hastings pseudo-Voigt parameters of the peak shape, scale factor, unit-cell parameters and atomic positions. Positional occupancy of all atoms and isotropic thermal factors were not refined.

The chemical composition of the samples was analyzed by the atomic emission spectroscopy applying the iCAP 6300 ICP (Thermo Scientific, USA) and OPTIMA 4300 DV (Perkin Elmer, USA) spectrometers. According to the obtained data, cation compositions of the samples correspond to theirs formulas. Lanthanum scandate oxides was found to have such impurities as calcium, potassium and silicium of less than 0.001, 0.001 and 0.002 atomic %, respectively.

Particle size distribution (PSD) of the samples was analyzed by laser scattering analysis using the Malvern Mastersizer 2000 (Malvern Instruments, United Kingdom). PSD results of $La_{1-x}Sr_xScO_{3-\delta}$ (x = 0, 0.04, 0.09) powder samples are shown in Fig. 1. The specific surface area was determined by BET method using Sorbi N.4.1 (Meta, Russia). Prior to measurement the samples were degassed during 1 h under the helium of 99.995% of purity flux at the temperature of 200 °C. The specific surface area of the $La_{1-x}Sr_xScO_{3-\delta}$ (x = 0, 0.04, 0.09) powder samples is shown in Table 1.

The Thermogravimetric Analysis (TGA) was performed on the powder samples (particle size is shown in Fig. 1) using the simultaneous thermal analyzer STA Jupiter 449 F1 (Netzsch, Germany) with water vapour generator Asteam DV2MK (Adrop, Germany). The so-prepared powder (sample mass 1.50 g) was heated up to 950 °C and held at this temperature during 8 h under the mixture of dry argon (99.998% of purity) and dry oxygen (99.999% of purity) to equilibrate the sample with the gas phase. Afterwards the carrier gas was saturated with water vapour (pH_2O = 0.24 atm, pO_2 = 0.18 atm) and then in the increase weight was recorded upon cooling from 950 °C to 300 °C with cooling

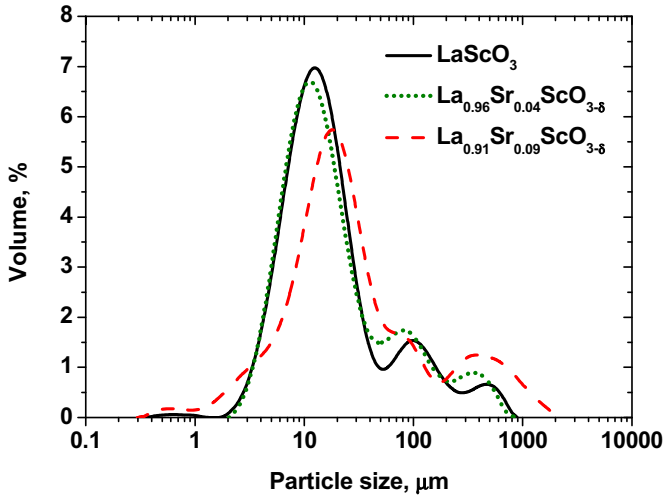

Fig. 1. Particle size distributions analysis of $La_{1-x}Sr_xScO_{3-\delta}$ (x = 0, 0.04, 0.09) powder samples.

Table 1
Specific surface area of $La_{1-x}Sr_xScO_{3-\delta}$ (x = 0, 0.04, 0.09) powder samples.

Chemical formula	$LaScO_3$	$La_{0.96}Sr_{0.04}ScO_{3-\delta}$	$La_{0.91}Sr_{0.09}ScO_{3-\delta}$
The specific surface area, m^2/g	0.64 ± 0.20	0.37 ± 0.20	0.89 ± 0.20

rate of 30 °C/h and 2 h of stabilization time at every 100 °C step. To release water from the crystal structure (dehydration procedure) before the TGA measurements the sample was dried in high vacuum with residual pressure of 10^{-9} atm at 950 °C for 1 h with the heating rate of 60 °C/h. This procedure was necessary in order to achieve the initial reproducible state for each sample. In order to eliminate the buoyancy effect of the balance of the thermal analyzer, the measured weight change was corrected by the result of the blank test without the sample in the crucible.

The NMR experiments were performed on the Avance III 500WB (Bruker, Germany) spectrometer at T = 300 K in the external magnetic field H_0 = 11.7 T. ^{45}Sc NMR spectra were obtained using standard spin-echo technique (τ–t_{del}–2τ–t_{del}–*echo*). The first pulse duration τ was equal to 2.2 μs. The delay between two successive pulses t_{del} was equal to 300 μs. Dry samples of $LaScO_3$ and $La_{0.91}Sr_{0.09}ScO_{3-\delta}$ were specifically prepared in order to avoid adsorption of water by the samples' surfaces from ambient air. All samples were dried in high vacuum by using the following method: a sample was placed into a quartz ampule in a furnace and heated to 950 °C with the heating rate of 60 °C/h under continuous pumping down by a turbo-molecular pump. After this the sample was fired in vacuum at 950 °C during 1 h. After thermogravimetric measurement the hydrated sample of $La_{0.91}Sr_{0.09}ScO_{3-\delta}$ was also placed in a quartz ampule and heated to 400 °C with the same heating rate and fired during 2 h to remove possible water from the surface of the specimen. After these procedures the quartz ampules were sealed.

3. Results and discussion

According to the XRD powder analysis pattern, shown in Fig. 2a, Sr-doped $LaScO_3$ oxides do not have any impurities. All the diffraction peaks of the $La_{1-x}Sr_xScO_{3-\delta}$ (x = 0, 0.04, 0.09) could be indexed as an orthorhombic perovskite unit cell (sp. gr. *Pnma*) that is in agreement with the literature [15–17]. Rietveld refinement of the XRD data of $La_{1-x}Sr_xScO_{3-\delta}$ (x = 0, 0.04, 0.09) confirms the phase purity of all samples (example of the data treatment of $La_{0.91}Sr_{0.09}ScO_{3-\delta}$ is shown in Fig. 2b). The results of Rietveld refinement are reported in Tables 2 and 3. As can be seen in Fig. 2a and Table 2, orthorhombic distortions